https://www.doi.org/10.53964/jmge.2022001

https://www.innovationforever.com

Journal of
Modern Green Energy

ISSN 2790-3206

Open Access

Research Article

An Estimation of the Performance of a Passive Cooling System Incorporating a Ground Heat Exchanger Using a Multilayer Artificial Neural Network

Hakan Tutumlu[1*], Erkan Duman[2], Mustafa Inalli[1]

[1]Department of Mechanical Engineering, Faculty of Engineering, University of Firat, Elazig, Turkey

[2]Department of Computer Engineering, Faculty of Engineering, University of Firat, Elazig, Turkey

[*]**Correspondence to: Hakan Tutumlu**, PhD, Research Assistant, Department of Mechanical Engineering, Faculty of Engineering, University of Firat, Elazig 23119, Turkey; E-mail: htutumlu@firat.edu.tr

Received: March 10, 2022 **Accepted:** June 9, 2022 **Published:** June 28, 2022

Abstract

Objective: This paper examines the cooling of an office building without a heat pump, using only ground heat exchangers (GHE) and implementing artificial neural network (ANN) to train it on experimental data.

Methods: The office building is situated at 38° 40′ 57″ N latitude and 39° 10′ 29″ E longitude in the province of Elazig. Each minute, the installed system was monitoring the office's external meteorological data, the office's indoor meteorological data, the GHE inlet and outlet temperatures, and the amount of heat load developed during the cooling process. In this study, the passive cooling system's cooling load and coefficient of performance (COP) were experimentally examined. A second important contribution of this paper is the multilayer ANN model that was created using data selected from the experimental setup, which was measured and recorded.

Results: During the summer months of 2018, the COP of the system was measured to be 1.67 on average. The accuracy rates of the multilayer ANN model proposed for cooling systems were calculated to be over 99% and 95% in the training and test datasets, respectively. It was observed that the performance value estimated by ANN converges to the true value by 99%.

Conclusion: Having performed this study, it has been demonstrated that passive cooling can be achieved with GHE, and by conducting this study without utilizing a heat pump system, we intend to contribute significantly to the relevant scientific literature.

Keywords: ground heat exchanger, passive cooling, multilayer artificial neural network, coefficient of performance estimation

Citation: Tutumlu H, Duman E, Inalli M. An Estimation of the Performance of a Passive Cooling System Incorporating a Ground Heat Exchanger Using a Multilayer Artificial Neural Network. *J Mod Green Energy*, 2022; 1: 1. DOI: 10.53964/jmge.2022001.

1 INTRODUCTION

It is imperative that we make use of energy that is efficient and, particularly, derived from renewable sources in order to reduce our impact on the environment[1]. Most of the energy used by the developed countries is provided from carbon-based sources such as fossil fuels and coal, which increase CO_2, SO_x and NO_x emissions[2]. For the purpose of reducing harmful emissions, national energy strategies of developed countries concentrate on finding new ways to access environmental, sustainable, and renewable energy sources[3]. As a result, the emission of gases that have grown in parallel with the global increase in energy demands has accelerated the search for alternative sources of energy. Among the renewable energy sources, geothermal energy has considerable potential for the nation of Turkey as a renewable, sustainable, and environmentally friendly source of energy[4]. Geothermal energy potential is extremely important in the processes of heating, cooling, and generating electricity. For cooling and heating processes carried out in conjunction with geothermal energy, heat exchanger technology has a great importance, especially in the case of ground heat exchangers. The main principle behind this energy source is based on the idea that the temperature of soil at a certain depth remains relatively constant throughout the year[5]. In the field of district heating, geothermal is considered one of the most promising renewable resources. The ground heat exchanger (GHE), which is buried underground at a certain depth, plays an important role in providing heat and cooling in the winter and summer, respectively. In summary, the underground can be used as a heat source and as a heat sink, thereby facilitating the ability to cool and heat[6]. There have been numerous studies demonstrating the efficiency of GHEs in both heating and cooling[7]. Ground-source heat pumps (GSHP) achieve optimal performance due to the thermal interaction of the pipes with the surrounding soil in addition to the surface area between the pipes and the soil[8]. For buildings, GHEs are generally used in conjunction with heat pumps for cooling and heating; such systems are called GSHPs[9]. Due to their high efficiency, ground source heat pumps paired with coaxial deep well heat exchangers are widely used[10]. The majority of research has focused on developing the machine structure in order to enhance the efficiency of GSHP. Nevertheless, in order to predict the performance of a proposed heating or cooling system, some parameters should be predicted during the design process before the system installation is undertaken. For such a prediction to be valid ahead of installation, it should be based on extensive experimental data such as the amount of greenhouse gas emissions, operating costs, system efficiency, life cycle, power consumption of the system, soil temperature, and exterior temperature[11].

Several studies have demonstrated that the temperature at the inlet, the circulating fluid velocity, the vertical pipe's center-to-center distance and the spiral pipe's higher pitch, as well as the thermal conductivity of the material in the filler are the factors influencing the system's performance[12]. This complex process is one of the most challenging in terms of obtaining data on the temperature and variation of underground soil, a factor that is paramount to making an informed assessment. Performance prediction with no system installation is extremely important, especially in heating and cooling applications involving large spaces. In engineering applications, artificial intelligence modeling techniques such as artificial neural networks (ANNs) are increasingly used to predict the performance of thermal systems[13]. Due to the accurate predictions obtained by modeling heat pump (HP) systems, cooling, heating, and air conditioning systems can be operated efficiently and maximum energy savings can be achieved. Particular importance should be attached to the prediction of the performance of HP systems utilizing underground temperatures[14]. Numerous studies have been conducted in regards to predicting the parameters of energy systems while they are in the planning stage; the most common means to do so is by using ANNs. An example of a study using ANN can be found here: Kalogirou predicted the intercept factor and local concentration ratio of a parabolic trough collector during the modeling and design of a solar powered steam generating plant. This study uses ANN to model and predict performance of solar-powered water heating systems[15]. A model based on ANNs, created by Bechtler in his study, has been used to analyze the continuous regime performance of a steam-compressed water source heat pump[16]. In order to model the steady-state performance of the steam compressed liquid cooler system, Swider assembled the ANN models that had been trained with similar experimental data to our study, and compared the results comprehensively[17]. The optimal design of a central heating system with a geothermal heat pump was achieved using a novel multi-layered ANN model described in Arat's study, another study conducted on the same topic as our own study[18]. Wang et al. developed an ANN model to predict the heat transfer resistance of a closed vertical-type laying, in which the liquid in the oscillating heat pipe is water. According to the authors, the purpose of the study was to provide a foundation for an oscillating heat pipe thermal resistance approach[19]. As part of an experimental investigation, Bilgiç et al investigated the Organic Rankine cycle. Input-output temperature values were determined using the mass flow of the evaporator and input-output temperature values were determined by analyzing the mass flow of cold fluids, and they were used for training an ANN network. By using the trained network, they were able to compare their predictions with the experimental results by predicting the power that Organic Rankine cycle generated[20]. An ANN model was developed by Azizi et al. to predict the heat transfer coefficient in an inclined tube using the cooling fluid R134a. This ANN is based on four input variables, namely inclination angle, mass flow, saturation temperature, and dryness fraction. An examination of the results of the ANN revealed that the rate of error in the accuracy of the model was less than 5%[21].

The purpose of this study was to determine whether ANN can be used and applied in predicting the performance of a passive cooling system with a ground heat exchanger. In order to accomplish this, a vertical U-type 104m borehole was used, and the polyethylene heat transfer pipes were installed in the borehole with a new approach. During the summer months, this cooling system was tested by cooling a $60m^2$ office. The outside meteorological data at 38° 40′ 57″ N latitude and 39° 10′ 29″ E longitude in Elazig province, where the office building is located, the indoor temperature values, and heat transfer amounts of the closed-loop passive cooling system were analyzed once per minute. In order to record data from the calorimeters, heat meters, and the meteorological station installed on the roof of the office building, we utilized an M-Bus data communication line. Based on this data, a thermodynamic analysis of this passive cooling system was formulated, as well as a mathematical-analytical model. In addition, an ANN that was trained using the datasets selected from a set of samples of real-world values measured and recorded was trained for this passive cooling system. On both the training and test datasets, the proposed ANN model achieved an accuracy rate of over 99% and 95%, respectively. Three different learning algorithms based on the back-propagation algorithm were selected for training the ANN model. There are three types of back-propagation algorithms: Levenberg-Marquardt (LM), pola-ribiere conjugate gradient (PRCG) and one-step-secant algorithm (OSS). With this ANN model, the instantaneous coefficient of performance of the passive cooling system was successfully predicted. ANN model developed in this study is very easy to use since it is made up of three input variables. Input variables for this model included the temperature values of brine entering and exiting the ground heat exchanger, as well as the cooling load of the office space. Using the forward propagation algorithm in the ANN, the estimated coefficient of performance (COP) value was calculated based on these input values. In the process of developing the ANN model, 70% of the data was used for training while the remaining 30% was used for testing and confirming its outputs. Following this research, the instantaneous COP values of the passive cooling system could be easily predicted using the developed ANN model. Observations have shown that the performance values of this system, which has been tested for the first time in the climate conditions of the province of Elazig, are positive.

In this study, which was conducted according to previous studies, an office was experimentally cooled at a depth of 105m without using any cooling equipment, only by using the earth itself as a heat sink. Furthermore, hourly performance calculations were made on the basis of hourly data. A system-specific multi-layer artificial intelligence system was also developed, and the ambient temperature, soil temperature, heat load, as well as the performance of the location under passive conditions were assessed without undergoing any experimental testing.

2 METHODS

2.1 Description of the Passive Cooling System

Figure 1 illustrates a schematic installation of the passive cooling system proposed. In Figure 2A are photographs of the installation of this system in the location (38° 40′ 57″ N latitude, 39° 10′ 29″ E longitude) of the Elazig province of Turkey. Figure 2B shows a view of the GHE positioned in the borehole drilled in the garden of the building.

Diagrams showing the schematic installation of passive cooling systems are shown in Figure 1, and photos showing examples of its actual application are shown in Figure 3. There are five main components of a passive cooling system, and these are: a vertical U-type GHE, a fan coil, a circulation pump, a cooling space, and a control unit. The installation may be summarized as follows:

As shown in Figure 3A, the GHE was placed vertically in the office garden, surrounded by filling material, and a fan-coil with a water-air heat exchanger was placed in order to provide space cooling. Through the fan coil, a closed circuit could be formed between the GHE and fan coil; in this closed circuit, the brine loop was operated by a very powerful circulation pump; a brine with an extremely high specific heat capacity was used in the closed circuit. Sensitive devices were used to perform measurements at the input-output of the GHE, at the fan-coil input-output, and at the pump input-output. During the recording process, the measurements were transferred to the control system shown in Figure 3B.

The GHE is the primary element of the passive cooling system, which transfers the waste heat energy drawn from the cooled office to the soil. A borehole is a cylindrical shaped well used for the installation of a geothermal heat exchanger. Underground temperatures fluctuate much less dramatically than those above ground. Underground temperatures remain constant within a given temperature range over the course of an entire year, which enables soil to become a great source of heat; the cooling system's COP increases as a result[22].

Under the ground, polyethylene (PE) pipes were employed as ground-water heat exchangers (Figure 4). In the borehole, the PE pipe employed as the GHE had a height and diameter of 104m and 21.59cm, respectively. The space between the borehole and the PE pipe was filled with concrete, a material with high thermal conductivity.

Figure 5 illustrates the pump that is used in the system. These include the following features: In single-phase models (220V), the motor has a thermal protector against overheating; It is resistant to dry running; It has a three-speed motor; and it works silently without any vibrations. In the following section, we describe in more detail the material characteristics of the NOVA circulation pumps. The impellers are techno polymer, the motor bodies are aluminum, and the motor shaft is ceramic. Due to the fact that the pump is cooled and lubricated by the fluid

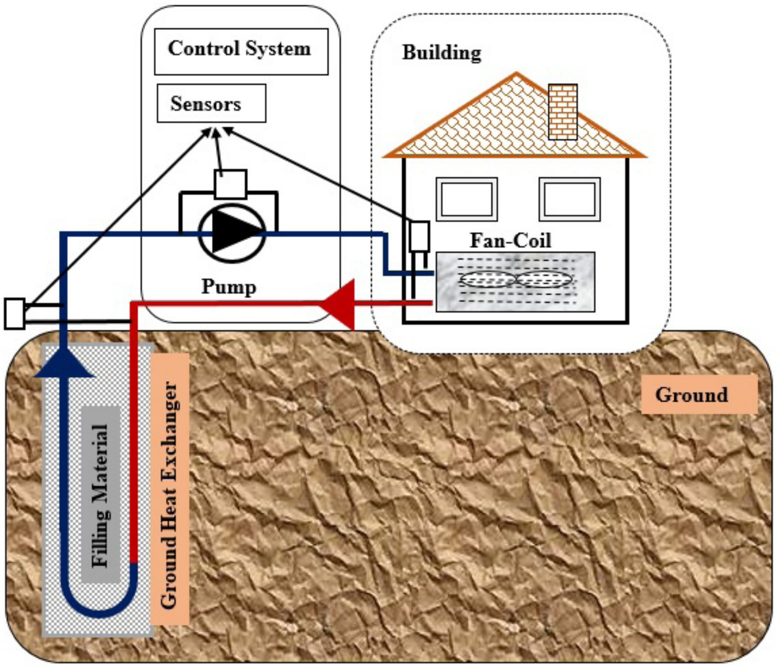

Figure 1. Schematic representation of a passive cooling system.

Figure 2. System installation location. A: Location of the office building; B: Office building of which passive cooling is done.

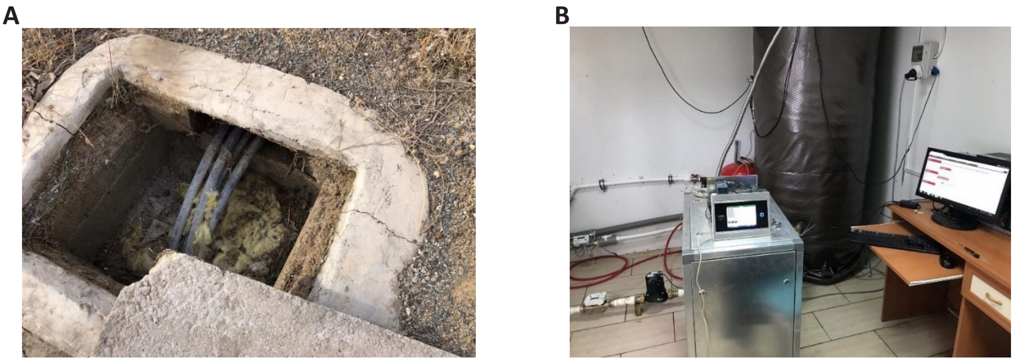

Figure 3. Practical application of passive cooling system. A: GHE; B: The cooled space and the control system.

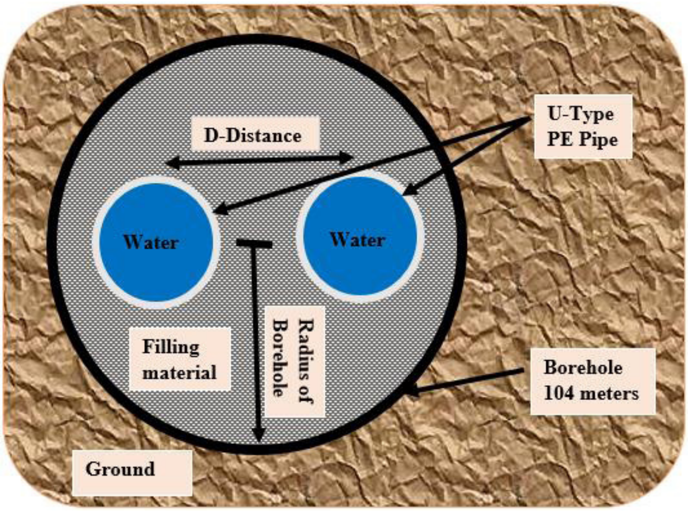

Figure 4. The straight section of the vertically positioned GHE.

it presses, it does not require an external engine cooling system; this type of boiler is typically used for heating capacities of up to 25,000kcal/h. Due to these features, the pump was chosen for use in a pipeline with a vertical length of 104m in a passive cooling system.

2.2 Thermal Analysis of the Passive Cooling System and Mathematical Model

As illustrated in Figure 6, the GHE was placed underground using a unique approach. As opposed to the classical design of having one entering-releasing heat pipe in the first 1.5m of soil depth and one line returning, a simple design was implemented that included two lines each in the first 1.5m and was reduced at the return to one line. The pipeline consisted of two hot brine release lines and two cold brine intake lines that entered the 1.5m depth, and as a result, the pipes had a larger surface area in contact with the soil. Consequently, the amount of heat emitted to soil increased, and this contributed to the high cooling coefficient of performance.

For the calculation of the thermal equilibrium of this passive cooling system with its environment as well as the cooling performance of the system, we used the equations of conservation of mass and energy. Both continuous flow and continuous regime conditions were utilized to model the analyzed system. In Tables 1 and 2 are the parameters of various types of ground and heat exchangers which were used in the thermal analyses are illustrated[23].

According to the laying in Figure 4, the laws of mass and energy conservation are represented in Equations (1) and (2). It is important to note that in a closed loop system the amount of mass entering the system and the amount of mass being released are equal for each device. Additionally, the amount of energy entering the system is equal to the amount of energy leaving the system under continuous regime conditions:

$$\sum \dot{m}_{in} = \sum \dot{m}_{out} \quad (1)$$

$$\dot{Q} + \sum \dot{m}_{in} \dot{h}_{in} = \dot{W} + \sum \dot{m}_{out} \dot{h}_{out} \quad (2)$$

It is important to note that if the kinetic and potential energy changes, as well as heat and work transfers, are ignored during the cooling period, the equilibrium turns into Equation (3):

$$\sum \dot{m}_{in} \dot{h}_{in} = \sum \dot{m}_{out} \dot{h}_{out} \quad (3)$$

We calculated the amount of heat energy that was emitted to the earth during the cooling process (GHE heat load, Q_H) using Equation (4)[24]:

$$Q_H = \dot{m}_w c_w \left(T_{3'} - T_{1'}\right) = UA_{up} \frac{T_{3'} - T_{1'}}{\ln\left(\frac{T_D - T_{1'}}{T_D - T_{3'}}\right)} \quad (4)$$

In this example, $\dot{m}_w$ and c_w represent the mass flow rate of brine from the closed loop with the GHE and the specific heat of the brine, respectively. Furthermore, A_{up}, U, T_D are defined as the heating surface area, the overall heat transfer coefficient, and the design temperature of the room, respectively. Following the above equation, the following relationship is obtained between the temperatures $T_{3'}$ and $T_{1'}$[24]:

$$T_{3'} = T_D - \left(T_D - T_{1'}\right) \exp\left(-\frac{UA_{up}}{\dot{m}_w c_w}\right) \quad (5)$$

The amount of the power consumption of the pump during the cooling process of the system (Pump, energy load, W_P) were calculated using Equation (6). Whilst, the amount of power consumed by the fan-coil (W_{fan}) was calculated using Equation (7):

$$W_P = \dot{m}_w \left(h_2 - h_1\right) = \dot{m}_w c \left(T_2 - T_1\right) \quad (6)$$

Figure 5. Pump used in passive cooling system.

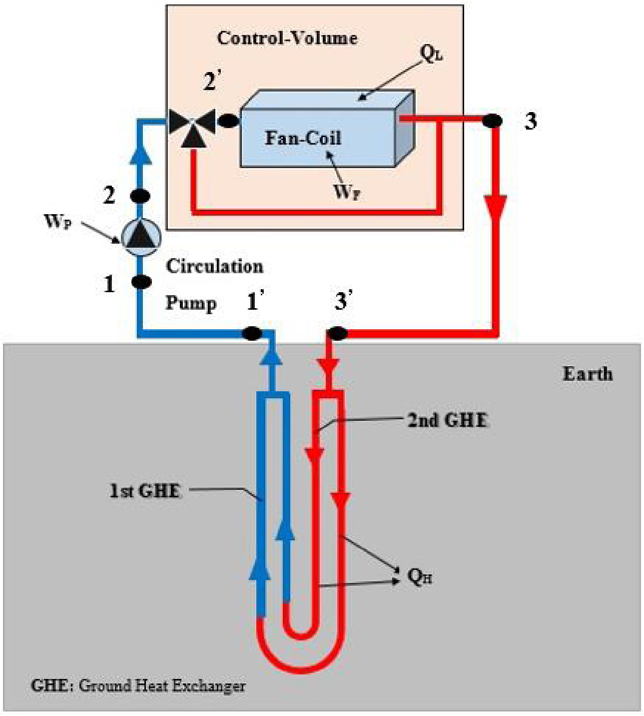

Figure 6. The schematic installation of the heat exchange of the passive cooling system.

Table 1. Parameters of Various Types of Ground

Type of Ground	Density [kg/m^3]	Thermal Conductivity [W(mK)]	Thermal Diffusivity [10-6m^2/s]	Specific Heat [J/(kgK)]
Sand/Gravel	1950	2.00	0.977	1050
Grained Ground	2000	0.52	0.141	1844

Table 2. Some Parameters of Passive Cooling System

Parameters	Values
Mass Flow Rate of Brine ($\dot{m}_w$)	0.2kg/s
Design Temperature (T_D) (For Summer Condition)	40^{o}C
Depth of GHE	104m
Storage Volume	4.35m^3
Borehole Depth	104m
Header Depth	1.5m

$$W_{fan} = \dot{m}_a\left(h_{3a} - h_{2a'}\right) = \dot{m}_a c_a\left(T_{3a} - T_{2a'}\right) \quad (7)$$

Where, c_a, T_{3a}, $T_{2a'}$, represent the mass flow rates of air from the fan coil, the specific heat of air, the input air temperature and the output air temperature to the fan coil, respectively.

The amount of heat absorption from the office by the fan coil during the cooling process of the system (cooling load due to fan-coil Q_L) was calculated using Equation (8):

$$Q_L = \dot{m}_w\left(h_3 - h_{2'}\right) = \dot{m}_w c\left(T_3 - T_{2'}\right) \quad (8)$$

The COP of the designed cooling system was calculated using Equation (9). Using a thermal analysis, a mathematical model was obtained and validated with actual system information.

$$COP_{\text{Passive Cooling}} = \frac{Q_H}{W_P + W_{Fan}} \quad (9)$$

3 RESULTS AND DISCUSSION

3.1 ANN Design for the Passive Cooling System

ANN is a mathematical model of the human nervous system, inspired by the neural network in the human brain and derived from the structure of human neurons with features such as learning, prediction and inference, even when there are incomplete data. In recent years, ANNs, which can predict given the relationship between interconnected cells, classify, and learn, have become one of the most popular optimization techniques in the evaluation of complex relationships[20].

An ANN is a network system based on the function of the brain and the structure of the brain, and is comprised of interconnected processing units, known as neurons[18]. An ANN is divided into three types of layers, these include: the input layer, one or more hidden layers, and output layer[19]. An important advantage of using ANNs is to create a practical model that engineers can use for solving problems and generating data. There are several important characteristics of ANNs, including the ability to store information relationally, gather information spatially, be robust, generalizable, and adaptable to learning, and have high parallelism[25].

ANNs are a very useful tool for modeling nonlinear functions. If enough training data is available, it is possible to predict nonlinear functions at a desired accuracy rate. As a result of their ability to predict nonlinear functions, ANNs have become invaluable tools for predicting nonlinear functions. Additionally, ANNs are quite capable of modeling complex correlations. An ANN can be used to model a system in three steps, as shown in the following example (Figure 7):

The process of learning in ANNs involves a constant updating of the weight vectors among the neurons; the results are optimized to cause the least amount of error. A training program's aim is to find the weight values so as to produce the right outputs for the samples that will be displayed in the network. The network is able to make generalizations about the event represented by the samples when the weight values are the appropriate ones. Network learning refers to this ability of the network to make generalizations. In the back-propagation algorithm, for the learning of the network, the weights are re-justified so as to decrease the difference between real outputs and predicted outputs. Figure 8 illustrates the structures and functions of the ANNs:

In addition, these values were also taught to the ANN to determine whether the performance prediction could be utilized without such a system being established. Figure 9 illustrates the ANN architecture that was created for the purpose of predicting the COP value of the proposed cooling system. The input variables of the ANN in the output layer were provided by selecting them from the recorded values of the system. According to Figure 9, in the proposed ANN model, the incoming-outgoing water temperatures (T1, T2) and the instant cooling load of the office were designed as the input variables of the ANN, and the COP of the passive cooling process was designed as the output variable.

By using the trial-and-error method, the number of hidden layers and the number of neurons in each layer was determined. The hidden layer of the network was initially composed of several neurons, which were gradually increased until the desired level of training error was achieved. In order to evaluate the error resulting from the difference between the real and predicted values, we calculated the mean square error (MSE), mean absolute relative error (MARE), and absolute change percentage (R^2). Accordingly, the R^2, MARE, and MSE error calculation methods are ranked in the following order[21]:

$$R^2 = \left[\frac{\sum_{i=1}^{n}\left(Y_{Pred,i} - \overline{Y}_{Pred}\right)\left(Y_{Exp,i} - \overline{Y}_{Exp,i}\right)}{\sqrt{\left(\sum_{i=1}^{n}\left(Y_{Pred,i} - \overline{Y}_{Pred}\right)^2\right)\left(\sum_{i=1}^{n}\left(Y_{Exp,i} - \overline{Y}_{Exp}\right)^2\right)}}\right]^2 \quad (10)$$

$$MARE = \left[\frac{1}{n}\sum_{i=1}^{n}\left|\frac{Y_{Exp,i} - Y_{Pred,i}}{Y_{Exp,i}}\right|\right] \times 100 \quad (11)$$

$$MSE = \frac{1}{n}\sum_{i=1}^{n}(e_i)^2 \quad (12)$$

Number of samples in the training dataset, predicted output values, experimental-real output values, and error values are represented, respectively, by n, Y_{Pred}, Y_{Exp}, ei. The $\overline{Y}_{Exp}$ value is the mean of the experimental values, and the $\overline{Y}_{Pred}$ value is the mean of the predicted values.

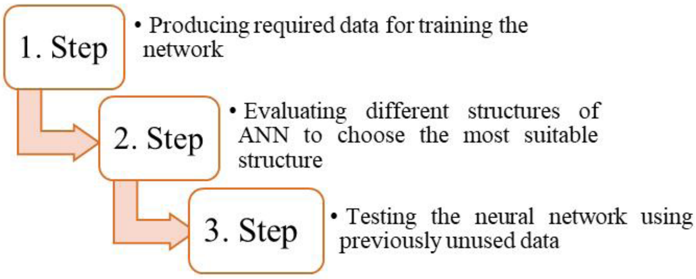

Figure 7. Steps to be followed in system modeling with ANN[26].

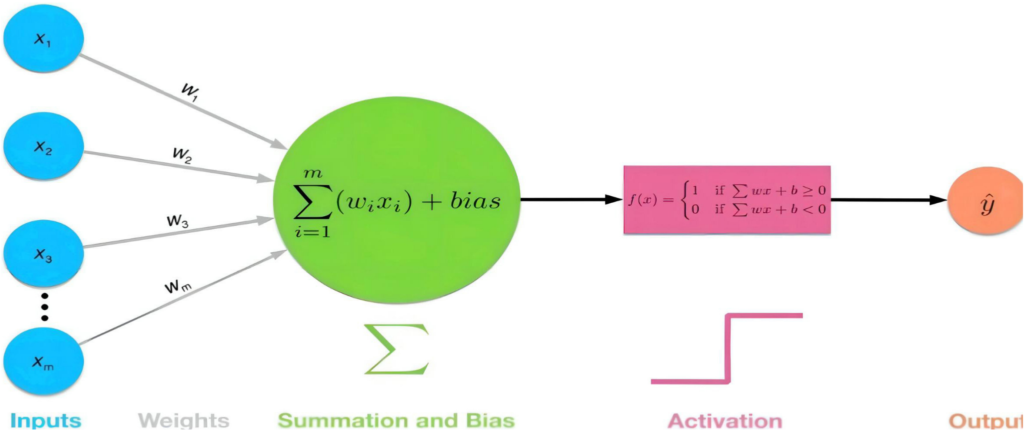

Figure 8. Functions and blocks of the ANN.

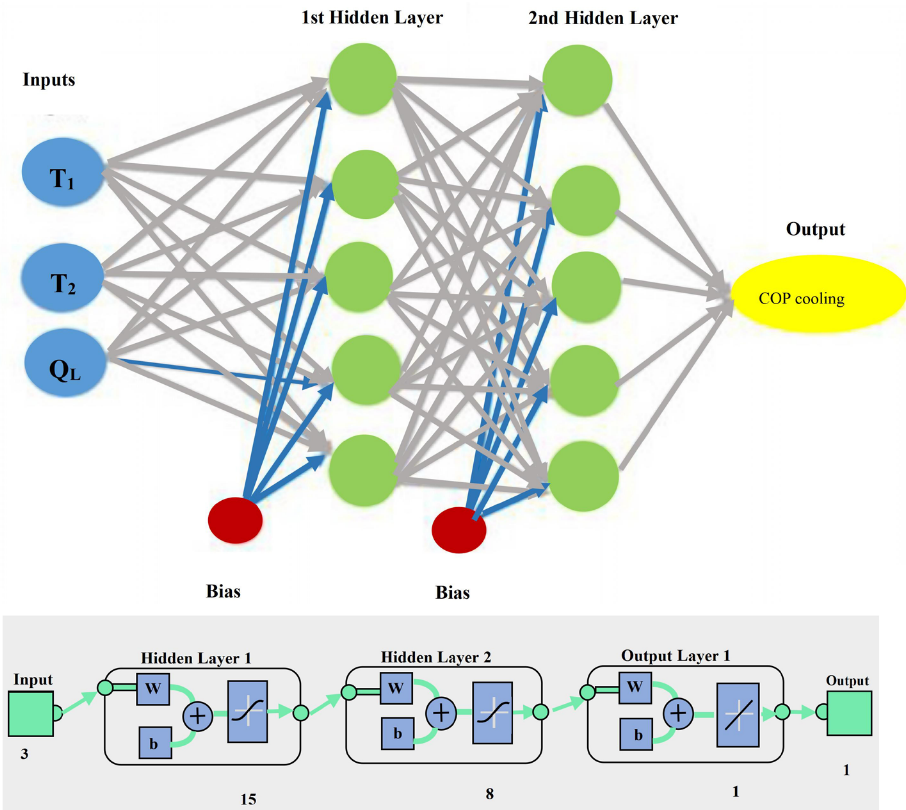

Figure 9. The multi-layered ANN architecture applied in this study.

A variety of alternative architectures with varying numbers of neurons in the hidden layer were tested using training data in order to determine the performances of the ANNs. The results of the study are presented in Table 3.

The R^2 method is a commonly used and reliable method in the literature for calculating R^2.

For the purpose of determining the optimal number of

Table 3. Accuracy Results of ANN Architectures with Different Numbers of Neurons and Hidden Layers

Number of Hidden Layers	Number of Neuron in Each Hidden Layer	R^2	MARE (%)	MSE
1	1	0.9969	1.0645	4.0565e-04
1	2	0.9969	1.0645	4.0652e-04
1	3	0.9969	1.0645	4.0636e-04
1	4	0.9969	1.0644	4.0616e-04
1	5	0.9969	1.0649	4.0710e-04
1	10	0.9969	1.0649	4.0683e-04
1	15	0.9970	1.0638	4.0447e-04
1	20	0.9948	1.1722	6.8877e-04
2	1	0.9969	1.0641	4.0569e-04
2	2	0.9969	1.0647	4.0665e-04
2	3	0.9969	1.0648	4.0666e-04
2	4	0.9969	1.0832	4.1527e-04
2	5	0.9969	1.0646	4.0607e-04
2	10	0.9971	1.0585	3.8887e-04
2	15	0.9945	1.1322	7.3191e-04
2	20	0.9957	1.1159	5.6587e-04

hidden layers and neurons, a trial-and-error method was used. Following the application of this method, the number of hidden layers was determined to be 2, the number of neurons in the first hidden layer was 15, and the number of neurons in the second hidden layer was 8. In order to model the proposed cooling system, this ANN architectural structure was used. Additionally, 2 levels of hidden layers were determined, and the impact of different learning algorithms and different numbers of neurons on statistical error varieties was examined and the results are shown in Table 4.

A conjugate gradient with Powell-Beale restarts algorithm (CGB) provides data updates for weights and deviations in a network. An algorithm like this is very useful for large-scale unconstrained optimization problems in ANNs. This is sometimes accomplished by resetting the search direction to the negative of the gradient. As soon as the number of mesh weights and deviations equals the number of iterations, the standard reset point is reached. However, there exists other approaches that can improve training efficiency, and one of these approaches is the Powell Beale restart method[12].

The OSS method attempts to bridge the gap between semi-Newton (secant) algorithms and conjugate gradient algorithms. As a result of this algorithm, the entire Hessian matrix is not stored; it assumes the identity matrix of the previous Hessian matrix upon each iteration. Furthermore, the new search direction can be calculated without having to calculate the inverse matrix[27].

This method employs the mathematical approach of the classical LM algorithm. The classical LM algorithm has proven to be very effective at learning small neural networks; this method becomes virtually inefficient for large neural networks, whose computational complexity increases significantly[28]. Therefore, this paper proposes local modification of the LM as a means of overcoming this limitation. Observation has shown that the best results are obtained using the LM algorithm.

10 days after the installation of the passive cooling system, hourly COP values were calculated by measuring parameter data such as temperature, mass flow, pressure, and power consumption. Figure 8 has been created based on these calculated values. As illustrated in Figure 10, the performance of the cooling system was observed to vary between 1 and 2. It can therefore be concluded that the passive cooling system is an effective means of cooling.

Our study examined whether there is a linear relationship between the predicted and measured COP values. The Figures 11 and 12 illustrate the correlation between the phases of training and testing; accordingly, the correlation value ranges from 0 to 1, and the closer the value is to 1, the more successful the network is[29]. Based on Figure 11, the correlation number of the network in the training was determined as 0,997; using the correlation value, the network's performance was mathematically proved to be successful.

As is seen in Figure 12, the error was calculated through the R^2 and the difference between experimental and predicted COP values. It was found that the ANN architecture created with the LM training algorithm had the highest similarity between experimental and predicted COP values.

Table 4. Cost Comparisons of Different Number of Neurons and Different Learning Algorithms

Algorithm	R^2	MARE (%)	MSE
LM-2	0.9956	1.0939	5.8200e-04
LM-3	0.9973	1.0088	3.5762e-04
LM-4	0.9958	1.1284	5.6186e-04
LM-5	0.9932	1.3587	9.0610e-04
LM-10	0.9955	1.1029	5.9348e-04
OSS-2	0.9671	3.1562	44.0000e-04
OSS-3	0.9930	1.5546	9.3044e-04
OSS-4	0.9812	1.8673	25.0000e-04
OSS-5	0.9802	1.8057	26.0000e-04
OSS-10	0.9218	4.8840	104.0000e-04
CGB-2	0.9886	1.4157	15.0000e-04
CGB-3	0.9756	2.8447	32.0000e-04
CGB-4	0.9895	1.2155	14.0000e-04
CGB-5	0.9908	1.6369	12.0000e-04
CGB-10	0.9792	1.9621	28.0000e-04

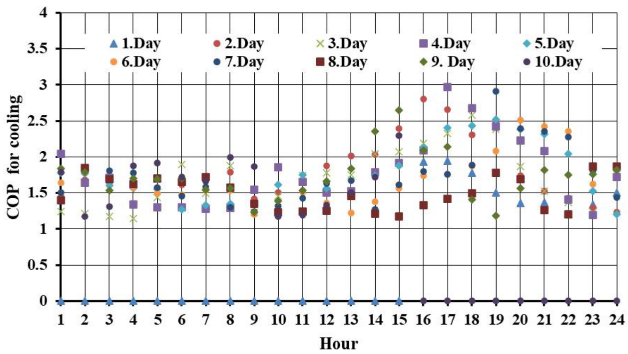

Figure 10. Hourly changes in the experimental COP values.

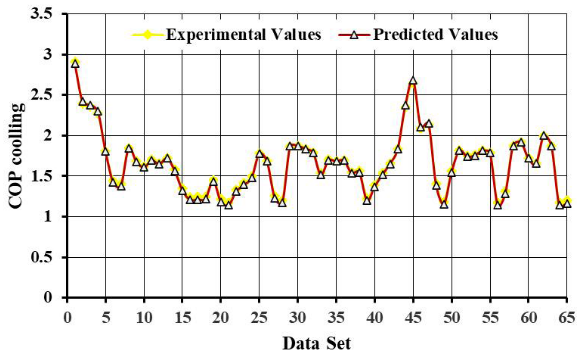

Figure 11. Comparison of the ANN-predicted and experimental COP values.

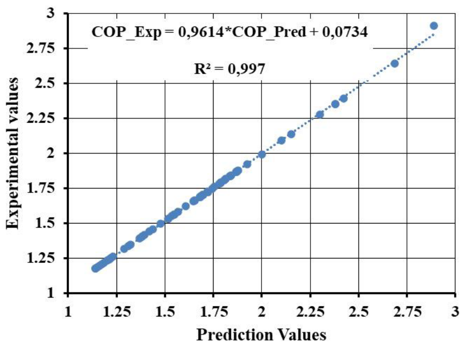

Figure 12. The correlation of the relationship between the ANN-predicted outputs and experimental COP values.

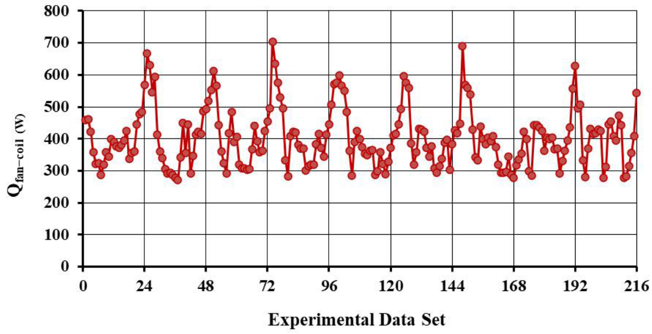

Figure 13. Experimentally determined hourly cooling load of the office.

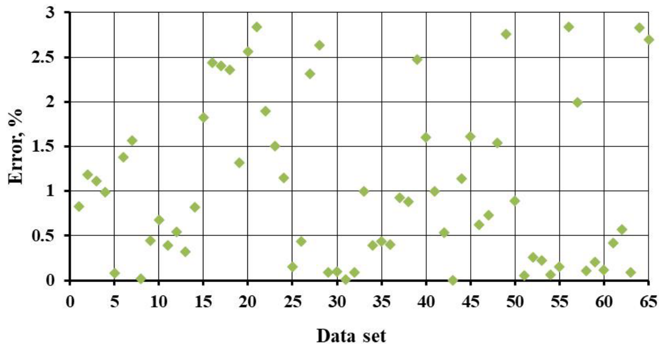

Figure 14. The percentage difference among error, ANN prediction, and experimental COP values.

Figure 13 demonstrates the change in cooling load of the office space on an hourly basis. Based on the figure, it can be seen that cooling load increases during the day and decreases during the night. In addition, these calculated cooling load values were utilized as target and prediction values during the training, ANN training, and the testing stages.

An absolute error rate was calculated between the COP values predicted by the ANN and the experimental COP values, and the results are shown in Figure 14. According to the figure, the change in error rate is between 0% and 3%. Based on these error rates, the accuracy of the description of the passive cooling system can be demonstrated.

4 CONCLUSION

The constantly increasing energy requirements of cooling, heating, and air conditioning systems warrant an increase in the use of renewable energy sources. However, the energy should be used as efficiently as possible through artificial intelligence techniques. In particular, for optimizing energy efficiency and productivity in these systems, ANNs can be utilized for parameter prediction. In this study, three different training algorithms were utilized in the ANN used to develop an optimization procedure for a cooling system with ground heat exchangers; it was determined that the LM algorithm provided the best performance for this system. The measurement of the brine entering and leaving the GHE, which are the input variables for the ANN, as well as the measurement of the cooling load of the office area, were experimentally conducted; the measured data was then used in the training, testing and verification stages of the ANN architecture. A correlation coefficient of 0.9973 was determined during the training of the network; the fact that the value is relatively close to 1 indicates the network's effectiveness. In this paper, the reaction of the network towards different datasets was examined and compared to the experimental outcomes. Based on the results of the comparison, the error rates were determined for each dataset, and the MSE error value was calculated as 1,008 as a result. In conclusion, it was found that the ANN developed for this cooling system performed well. Through the use of this ANN, the COP predictions are made to be in line with reality without the need to rely on multiple GHE systems. Accordingly, it was understood that the system parameters could be adjusted based on ANN predictions, and that cooling performance analysis could be completed. Finally, the performance values of the passive cooling system with ground heat changer, which was tested initially in Elazig province's climatic conditions, were found to be quite satisfactory. As a result, it has been observed that in the passive cooling process, the performance coefficient varies between 1.2 and 2.5. Furthermore, it has been determined that soil can be used as a heat sink to produce exemplary results.

Acknowledgements

This study was conducted within the framework of the FÜBAP-MF.17.23 Project and was supported financially by the Firat University Scientific Research Projects Management Department.

Conflicts of Interest
The authors had no conflict of interest to disclose.

Author Contribution
All authors contributed to the manuscript and approved the final version.

Abbreviation List
ANN, Artificial neural network
A_{up}, Heating surface area of the ground heat exchanger
c_a, Specific heat of air
CGB, Conjugate gradient with powell/beale restarts algorithm
COP, Coeffiecient of performance
c_w, Specific heat of brine
D, Design
e_i, Error values
Exp, Experimental
GHE, Ground heat exchanger
GSHP, Ground source heat pump
HP, Heat pump
i, Number of set
LM, Levenberg-Marquardt algorithm
$\dot{m}_a$, Mass flow rate of air from fan-coil
MARE, Mean absolute relative error
MSE, Mean square error
$\dot{m}_w$, Mass flow rate of brine
n, Number of samples in the training dataset
OSS, One-step-secant algorithm
Pred, Prediction
$Q_{fan\ coil}$, Experimentally determined hourly cooling load of the office
R^2, Absolute change percentage
$T_{1'}$, Output temperature of brine from ground heat exchanger
$T_{2a'}$, Temperature of output air from fan-coil
$T_{3'}$, Input temperature of brine to ground heat exchanger
T_{3a}, Temperature of input air to fan-coil
T_D, Design temperature (for summer condition)
U, Overall heat transfer coefficient
$\bar{Y}_{Exp}$, Mean of experimental values
$\bar{Y}_{Pred}$, Mean of predicted values
Y_{Pred}, Predicted output values

References

[1] Nicoletti G, Arcuri N, Nicoletti G et al. A technical and environmental comparison between hydrogen and some fossil fuels. *Energ Convers Manage*, 2015; 89: 205-213. DOI: 10.1016/j.enconman.2014.09.057
[2] Ediger VŞ, Kentel E. Renewable energy potential as an alternative to fossil fuels in Turkey. *Energ Convers Manage*, 1999; 40: 743-755. DOI: 10.1016/S0196-8904(98)00122-8
[3] Kuyumcu ME, Tutumlu H, Yumrutaş R. Performance of a swimming pool heating system by utilizing waste energy rejected from an ice rink with an energy storage tank. *Energ Convers Manage*, 2016; 121: 349-357. DOI: 10.1016/j.enconman.2016.05.049
[4] Develioğlu M. Technological developments of ground source heat pumps and application possibilities in Turkey. Master Thesis at Hacettepe University, 2012.
[5] Ceylan H. Experimental Study on the Change of Ground Heat Exchanger Length with Condenser Temperature. *Energy Machinery*, 2017; 58: 39-51.
[6] Gao J, Li A, Xu X et al. Ground heat exchangers: Applications, technology integration and potential for zero energy buildings. *Renew Energ*, 2018; 128: 337-349. DOI: 10.1016/j.renene.2018.05.089
[7] Esen H, Inalli M. In-situ thermal response test for ground source heat pump system in Elazig, Turkey. *Energ Buildings*, 2009; 41: 395-401. DOI: 10.1016/j.enbuild.2008.11.004
[8] Farajollahi AH, Asgari B, Rostami M. Thermal performance analysis of an energy pile with triple helix ground heat exchanger. *Geothermics*, 2022; 104: 102459. DOI: 10.1016/j.geothermics.2022.102459
[9] Esen H, Inalli M. ANN and ANFIS models for performance evaluation of a vertical ground source heat pump system. *Expert Syst Appl*, 2010; 37: 8134-8147. DOI: 10.1016/j.eswa.2010.05.074
[10] Wang Y, Wang Y, You S et al. Operation optimization of the coaxial deep borehole heat exchanger coupled with ground source heat pump for building heating. *Appl Therm Eng*, 2022; 213: 118656. DOI: 10.1016/j.applthermaleng.2022.118656
[11] Esen H, Inalli M, Sengur A et al. Predicting the performance of a ground-source heat pump system using fuzzy weighted pre-processing-based ANFIS. *Build Environ*, 2008; 43: 2178-2187. DOI: 10.1016/j.buildenv.2008.01.002
[12] Adedayo OO, Onibonoje MO, Fabunmi TE. Simulative Analysis of Metropolitan Electric Distribution Network using Conjugate Gradient Neuro-algorithm with Powell/Beale Restarts: 2021 International Conference on Electrical, Computer and Energy Technologies (ICECET), Cape Town, South Africa, 09-10 December 2021. IEEE Xplore; 2021. DOI: 10.1109/ICECET52533.2021.9698441
[13] Nagano K, Katsura T. Performance prediction program and performance prediction system for a ground source heat pump system. US Pat 7,113,888, 2006.
[14] Esen H. Investigation of seasonal behaviour of a vertical ground source heat pump used in residential air conditioning systems [PhD thesis]. Elazig, Turkey: University of Firat; 2007.
[15] Kalogirou SA. Applications of artificial neural-networks for energy systems. *Appl Energ*, 2000; 67: 17-35.
[16] Becthler H, Browne MW, Bansal PK et al. Neural networks-A new approach to model vapour-compression heat pumps. *Int J Energ Res*, 2001; 25: 591-599. DOI: 10.1002/er.705
[17] Swider DJ. A comparison of empirically based steady-state models for vapor-compression liquid chillers. *Appl Therm Eng*, 2003; 23: 539-556. DOI: 10.1016/S1359-4311(02)00242-9
[18] Arat H, Arslan O. Optimization of the district heating system aided by geothermal heat pump: a novel multistage with multilevel ANN modelling. *Appl Therm Eng*, 2017; 111: 608-623. DOI: 10.1016/j.applthermaleng.2016.09.150
[19] Wang X, Li B, Yan Y et al. Predicting of thermal resistances of closed vertical meandering pulsating heat pipe using artificial

neural network model. *Applied Thermal Engineering*, 2019; 149: 1134-1141. DOI: 10.1016/j.applthermaleng.2018.12.142
[20] Bilgiç HH, Yagli H, Ali KOC et al. Power Prediction with Artificial Neural Network in Experimental Organic Rankine Cycle. *Selcuk Uni J Eng Sci Technol*, 2016; 4: 7-17. DOI: 10.15317/Scitech.2016116091
[21] Azizi S, Ahmadloo E. Prediction of heat transfer coefficient during condensation of R134a in inclined tubes using artificial neural network. *Appl Therm Eng*, 2016; 106: 203-210. DOI: 10.1016/j.applthermaleng.2016.05.189
[22] Yumrutaş R, Ünsal M. Analysis of solar aided heat pump systems with seasonal thermal energy storage in surface tanks. *Energy*, 2000; 25: 1231-1243. DOI: 10.1016/S0360-5442(00)00032-3
[23] Ozisik MN. Heat Transfer: A Basic Approach. McGraw-Hill: New York, USA, 1985.
[24] Larwa B, Kupiec K. Temperature profiles in ground heat exchangers. *Tech T Chem*, 1-Ch/2014.
[25] Ahmadloo E, Azizi S. Prediction of thermal conductivity of various nanofluids using artificial neural network. *Int Commun Heat Mass*, 2016, 74: 69-75. DOI: 10.1016/j.icheatmasstransfer.2016.03.008
[26] Esfe MH, Wongwises S, Naderi A et al. Thermal conductivity of Cu/TiO2-water/EG hybrid nanofluid: Experimental data and modelling using artificial neural network and correlation. *Int Commun Heat Mass*, 2015; 66: 100-104. DOI: 10.1016/j.icheatmasstransfer.2015.05.014
[27] Constantinescu R, Lazarescu V, Tahboub R. Geometrical form recognition using 'One-Step-Secant'algorithm in case of neural network. *UPB Sci Bull Ser C*, 2008; 70: 15-28.
[28] Bilski J, Kowalczyk B, Marchlewska A et al. Local Levenberg-Marquardt algorithm for learning feedforwad neural networks. *J Artif Intell Soft*, 2020; 10: 299-316. DOI: 10.2478/jaiscr-2020-0020
[29] Dogan E, Ates A, Yilmaz EC et al. Application of artificial neural networks to estimate wastewater treatment plant inlet biochemical oxygen demand. *Environ Prog*, 2008; 27: 439-446. DOI: 10.1002/ep.10295